Limits on the validity of infinite length assumptions for modelling shallow landslides

Journal:	*Earth Surface Processes and Landforms*
Manuscript ID:	ESP-11-0234.R1
Wiley - Manuscript type:	Paper
Date Submitted by the Author:	14-Dec-2011
Complete List of Authors:	Milledge, David; Durham University, Institute of Hazard Risk and Resilience; Durham University, Department of Geography Griffiths, D; Colorado School of Mines, Division of Engineering Lane, Stuart; Université de Lausanne, Institut de géographie Warburton, Jeff; Durham University, Department of Geography
Keywords:	infinite slope length, stability model, shallow landslide, finite element method, benchmark

Limits on the validity of infinite length assumptions for modelling shallow landslides

Abstract

The infinite slope method is widely used as the geotechnical component of geomorphic and landscape evolution models. Its assumption that shallow landslides are infinitely long is usually considered valid for natural landslides on the basis that they are generally long relative to their depth. However, this is rarely justified because we lack a clear definition of the critical length / depth ratio below which edge effects become important and length dependence appears. Here we benchmark infinite slope predictions across the range of possible slope properties found on natural slopes to establish the critical length at which infinite slope stability predictions fall within 5 and 10% of those estimated by a finite element method. We find that infinite slope stability predictions always converge to within 5% of the finite element benchmarks at a critical length / depth ratio of 25. However, they can converge at much lower ratios depending on slope properties, particularly the proportions of cohesive versus frictional soil strength so that critical length depth ratios are smaller for low cohesion soils. As a result the infinite length assumption within the infinite slope method is valid for catchment scale models when their grid resolution is coarse (e.g. >25 m). However, it may also be important when their grid resolution is much finer, because spatial organisation in the predicted pore water pressure field reduces the probability of short landslides and minimises the risk that predicted landslides will have length / depth ratio's less than 25.

Keywords: infinite slope length, stability model, shallow landslide, finite element method, benchmark.

Background

Shallow landslides are important agents of erosion and sources of sediment in terrestrial environments and need to be represented in geomorphic (e.g. Montgomery and Dietrich, 1994; Bathurst *et al*., 2005; Reid *et al*., 2007) and landscape evolution models (e.g. Tucker and Bras, 1998), However, a full stability analysis at every potential landslide site is not feasible; therefore much work has focussed on trying to develop simple physically based methods to identify shallow landslide risk comparatively across the landscape (e.g. Montgomery and Dietrich, 1994; Baum *et al*., 2008).

The infinite slope method (Taylor, 1948; Haefeli, 1948; Skempton and DeLory, 1957) is widely used as the geotechnical component of these geomorphic and landscape evolution models where it is generally combined with a hydrological model to predict pore water pressure and hence failure probability. Much attention in developing these models has been focussed on different approaches to predicting the spatial pore water pressure patterns (Montgomery and Dietrich, 1994; Burton and Bathurst, 1995; Wu and Sidle, 1995; Reid *et al*., 2007; Simoni *et al*., 2008; Baum *et al*., 2008). However, much less attention has been given to the geotechnical component. This is partly because the assumptions behind the infinite slope method, particularly of infinite width and length (Skempton and DeLory, 1957), are considered valid for many natural landslides, which have relatively high length (L) / depth (H) ratios (Haneberg, 2004). Furthermore, attempts to account for the influence of the landslide margins on the balance of forces requires additional assumptions to be made about the location, orientation, and magnitude of the forces involved.

The argument that the infinite slope method is suitable for shallow landslides because they have high length / depth (L/H) ratios is frequently stated but rarely justified (Wu and Sidle, 1995; Iverson, 2000; Crosta and Frattini, 2002; Casadei *et al*., 2003; Haneberg, 2004; Bathurst *et al*., 2005; Ray *et al*., 2010). Most natural landslides are shallow, Figure 1 shows two example inventories where L/H ratios exceed 7 for >90% of landslides (Gabet and Dunne, 2002; Warburton *et al*., 2008), while the

scaling analysis of Larsen *et al*. (2010) suggests *L/H* ratio increases with length ($L/H = 12.5\ L^{0.16}$) and exceeds 18 even for very small landslides (L<4 m). However, we cannot assume that the infinite slope method is suitable for these landslides without more rigorous testing. This requires an assessment of the *L/H* ratio of the predicted or observed landslides relative to the *L/H* ratio at which infinite slope assumptions break down.

<Figure 1 near here>

Recent work by Griffiths *et al*. (2011) has begun to address this by benchmarking infinite slope predictions against those from a finite element (FE) continuum mechanics method. The rationale for this is that the FE predictions can be assumed as a benchmark for the stability of a given slope. This is reasonable since they have been shown to be reliable and robust for assessing the factor of safety of slopes across a range of scenarios (Griffiths and Lane, 1999). They perform at least as well as limit equilibrium methods for known parametric tests (Hammah *et al.*, 2005) but are far more flexible, not requiring assumptions about: the shape or location of the failure surface, nor the inter-slice forces (Griffiths and Lane, 1999). On this basis, infinite slope stability predictions can then be tested against the FE predictions for different slope lengths.

Griffiths *et al*. (2011) find that the FE predictions converge on those from the infinite slope method at *L/H* ratios of around 16 and suggest that, in general, the infinite slope method is suitable for *L/H* > 16. However they show that for slopes with shorter *L/H* ratios the infinite slope method predictions become increasingly different to the benchmark as *L/H* decreases. At an *L/H* ratio of two, the infinite slope method can predict that a slope is less than half as stable as the FE method predicts for the same slope. They attribute this difference to error in the infinite slope method resulting from the violation of its infinite length assumption. This has potentially significant implications for the appropriateness of the infinite slope method for geomorphic modelling. Such models often rely on cell-by-cell calculations of infinite-slope stability with resolutions ranging from a few to tens of meters. The often implicit assumption in applying these models is that the grid cells are adequately

long relative to the landslide failure plane depth so that factors of safety calculated with an infinite slope approach are reasonably free of error. If the findings of Griffiths *et al*. (2011) hold across the full range of natural slope conditions then this assumption would be valid for models with grid cells longer than 16 times the assumed failure plane depth but could introduce error at finer resolutions. In this paper we extend some of the initial conclusions from Griffiths *et al*. (2011) to establish the generality of their findings; then assess the implications of these findings for stability analysis within geomorphology and landscape evolution models.

The Infinite Slope Method

The most common geotechnical measure of slope stability is the factor of safety (*FoS*) the ratio of shear strength of the soil (s) to the shear stress (τ) required for equilibrium.

Equation 1

$$FoS = \frac{s}{\tau}$$

A slope is considered to be just stable when the stresses and strengths are equal and the *FoS* is equal to one and to fail for $FoS < 1$. The factor of safety can be calculated using a range of approaches, including the one dimensional infinite slope method, and more sophisticated limit equilibrium and continuum mechanics methods in two and three-dimensions. More sophisticated methods allow improved representation of the failure geometry. However, they require fine scale discretisation of the slope, phreatic surface and failure plane geometries and generally need to be solved iteratively. These data and computational requirements limit their applicability at the catchment scale where analysis almost invariably involves the simpler one-dimensional infinite slope method.

<Figure 2 near here>

The Infinite Slope (IS) method (Taylor, 1948; Haefeli, 1948; Skempton and DeLory, 1957) makes two key assumptions: 1) that sliding occurs along a pre-defined plane parallel to the face of the slope; and 2) that the sliding block is infinitely long and wide so that stresses are the same on the two

planes perpendicular to the slope (e.g. stresses A-A' = stresses B-B' in Figure 2). These stresses are collinear, equal in magnitude and opposite in direction. Therefore they exactly balance each other and can be ignored. The equilibrium equations are derived using a rectangular block (e.g. A-B-B'-A'). All the stresses perpendicular (σ) and parallel (τ) to the failure plane are summed to give:

Equation 2

$$\tau = W \sin\beta = \gamma_s H \cos\beta \sin\beta$$

Equation 3

$$\sigma = \cos\beta W = \cos^2 \beta \gamma_s H$$

where: β is the block's slope [-]; W is the weight of the block [kN]; σ is the normal stress on the slip plane [kPa]; γ_s is the soil unit weight [kN m^{-3}]; and H is the vertical depth to the shear plane [m]. Assuming steady seepage parallel to the slope at a depth of H_w above the failure plane [m], we can account for the effect of pore water pressure (u) [kPa] on normal stress to calculate the effective normal stress using:

Equation 4

$$\sigma - u = \cos^2 \beta(\gamma_s (H - H_w) + (\gamma_s - \gamma_w) H_w) = \cos^2 \beta H(\gamma_s - \gamma_w m)$$

where: γ_w is the water unit weight [kN m^{-3}]; and m is the normalised free surface height [-] defined as $m=H_w/H$; m=1 for fully saturated flow with the phreatic surface at the ground surface, and m=0 for "dry" cases where the phreatic surface is below the failure plane and does not affect the stability. Shear strength (s) [kPa] for effective stresses is expressed by the Mohr–Coulomb equation as:

Equation 5

$$s = c' + (\sigma - u)\tan\varphi'$$

where: c' is the effective soil cohesion [kPa]; and φ' is the effective friction angle [-]. Substituting Equation 2, Equation 3 and Equation 5 into Equation 1 to calculate the factor of safety (FoS) [-] gives:

Equation 6

$$FoS = \frac{c' + \cos^2 \beta H(\gamma_s - \gamma_w m)\tan\varphi'}{\gamma_s H \cos\beta \sin\beta}$$

This provides a very simple one-dimensional balance of forces equation for slope stability that can be easily applied within a spatial model for landslides since the stability of each element can be calculated independent of its neighbours.

However, its validity and predictive ability is defined by the extent to which its assumptions are met. Griffiths *et al*., (2011) have suggested that the infinite length assumption is reasonable for *L/H* ratios greater than 16. However, before we can use this as a critical *L/H* ratio when assessing the suitability of the infinite slope method for catchment modelling we need to know: 1) how general this result is under the range of plausible conditions found in natural landscapes; and 2) which slope properties, if any, influence the magnitude of the critical *L/H* ratio.

Method

Parameter exploration

To address these questions we explored the influence of *L/H* ratio on the accuracy of the infinite slope method by benchmarking it against the same finite element method as Griffiths *et al*. (2011). To establish the generality of the relationships we varied all the other parameters within the infinite slope equation (Equation 6, cohesion, friction angle, soil depth, normalised free surface height, soil unit weight and slope angle). We varied these parameters across their reasonable ranges (Table 1) and assessed the impact of these variations on the critical *L/H* ratio (L/H_{crit}) at which the infinite slope predictions converged with those from the finite element method.

Our experimental design for the parameter exploration had two components. First, we used a systematic parameter exploration to test the method's performance for a set of extreme parameter combinations at the limits of the parameter space. The parameters and their limits are listed in Table 1. In each case we used the FE method to predict *FoS* at *L/H* ratios of: 4, 8, 12, 16, 24 and 48. These ratios were chosen after initial tests in order to sample most densely in the region of expected convergence for the two methods but with some samples at longer *L/H* ratios to ensure that any extreme responses were captured. We then compared the FE and IS predictions, standardising the results by expressing the difference between predictions as a percentage of the FE *FoS*. The systematic parameter exploration is useful in illustrating the form of the *FoS* difference curves across

the reasonable range of slope properties. However, it is difficult to interpret in terms of the influence of individual parameters on the L/H_{crit} value because: 1) it only shows results for the extreme limits to the slope properties; and 2) the parameter combinations are difficult to differentiate.

Second, we addressed the limitations above using a random parameter exploration. Here, we applied a Monte Carlo approach, sampling each of the six infinite slope parameters randomly and assuming a uniform distribution across the range defined in Table 1. Although some of the parameters in the IS method tend to co-vary (e.g. φ' and c') we sampled from uniform distributions and avoided *a priori* assumptions about their covariance because we were interested in the sensitivity of the method to the full range of possible conditions and so needed broad and uniform coverage of the parameter space. This generated 5000 synthetic slopes with random slope geometry and material properties. For each of these we then calculated stability using the FE and IS methods for the same set of *L/H* ratios used in the first parameter exploration. Again the error in the IS predictions was expressed as a percentage of the FE *FoS*. The L/H_{crit} at which the FE method converged to within 5% and 10% of the IS predictions was recorded. These critical *L/H* ratios could then be plotted against each parameter to show the influence of that parameter on L/H_{crit}. The systematic tests (from the first step) could be used to ensure that the extremes of the parameter ranges have been sampled and to ensure confidence in our assertion about the maximum *L/H* ratio required to satisfy the infinite slope assumptions. Both the systematic and Monte Carlo explorations involved modifying the parameters in combination (as opposed to one at a time) to account for interaction effects between parameters.

<Table 1 near here>

Finite Element method

To benchmark the infinite slope predictions for slopes of a defined length, we compare them with a finite element method developed by Griffiths and Lane (1999) and modified by Griffiths *et al.* (2011) to make it suitable for landslides on long slopes with very high *L/H* ratios. The method has been validated against the infinite slope method for scenarios where the FE domain simulates infinite

length conditions (Griffiths *et al*., 2011, Sections 4 and 5). The model performs 2D plane strain analysis of elastic-perfectly plastic soils with a Mohr-Coulomb failure criterion using 8-node quadrilateral elements with reduced integration (4 Gauss-points per element) in the gravity loads generation, the stiffness matrix generation and the stress redistribution phases of the algorithm. The soil is initially assumed to be elastic and the model generates normal and shear stresses at all Gauss-points within the mesh. These stresses are then compared with the Mohr-Coulomb failure criterion. If the stresses at a particular Gauss-point lie within the Mohr-Coulomb failure envelope then that location is assumed to remain elastic. If the stresses lie on or outside the failure envelope, then that location is assumed to be yielding. Yield stresses are redistributed throughout the mesh using the visco-plastic algorithm (Perzyna 1966, Zienkiewicz *et al*. 1975). Overall shear failure occurs when a sufficient number of Gauss-points have yielded to allow a mechanism to develop. The factor of safety is defined as the ratio of the average shear strength of the soil to the average shear stress developed along the critical failure surface and is calculated using the shear strength reduction technique (Zienkiewicz *et al*., 1975).

The domain geometry and boundary conditions are designed to represent slopes of a finite length. They should be simple enough to isolate the effect of length on stability but representative so that we can be confident that our conclusions apply to natural slopes. We use a mesh of 8-noded quadrilateral elements (shown in Figure 3). The mesh consists of horizontal sections to the left and right, and a long sloping central section. The base of the mesh is fully fixed and the extreme vertical boundaries to the left and right allow vertical movement only. This simple representation of a finite slope, with a sloping section between two horizontal sections, is common in slope stability modelling (Chugh, 2003). The boundary conditions on the base are exactly the same as in the IS method in that shearing can occur at the base of the soil layer. We chose fixed rather than periodic vertical boundaries since we are interested in the IS method's ability to represent finite slopes. We added horizontal sections 4 times the domain depth and allowed vertical movement on the vertical boundaries to minimize edge effects. The size of real landslides is defined not only by a slope's geometry but also its pore water pressure and material properties, which vary across the slope. This

variability might be responsible for defining the unstable part of a slope but cannot be represented within the IS method. The simplest way of creating a zone of decreased stability between two more stable zones is to change the domain geometry at the head and toe. In this respect we are changing the geometry to create more stable regions and ensure that the failure is a finite (defined) length. We tested end sections inclined at a range of angles but found that for sloping end sections the failure can expand to fill the full domain. This increases the influence of the vertical boundary conditions and alters the geometry of the failure plane so that it is no longer consistent with the IS method. We chose horizontal sections for consistency and simplicity. This represents both the specific case of a finite slope with uniform material properties and horizontal sections above and below it and the more general case of a slope with more stable zones above and below it. Our tests using a sloping end sections showed that where the failure was limited to the sloping section change in inclination of the end sections lead to only minor changes in predicted stability.

<Figure 3 near here>

We represent the slope geometry and soil properties using the six parameters shown in Table 1 with elastic parameters Young's modulus and Poisson's ratio, which are needed by the displacement-based FE formulation to introduce stresses into the model. These elastic parameters have been shown to have little influence on stability predictions (Hammah *et al*., 2005) and are held constant throughout the study at nominal values of 10^5 kPa and 0.3 respectively.

The FE model has one further soil parameter, the dilation angle, which affects the volume change of the soil during yielding. It is well known that the actual volume change exhibited by a soil during yielding is quite variable. For example a medium dense material during shearing might initially exhibit some volume decrease ($\psi < 0$) followed by a dilative phase ($\psi > 0$), leading eventually to yield under constant volume conditions ($\psi = 0$). Clearly this type of detailed volumetric modelling is beyond the scope of the elastic-perfectly plastic models used in this study where a constant dilation angle is implied. The question then arises as to what value of ψ to use. If $\psi = \varphi$ then the plasticity

flow rule is 'associated' and direct comparisons with theorems from classical plasticity can be made. In spite of this potential advantage, it is also well known that associated flow rules with frictional soil models predict far greater dilation than is ever observed in reality. This in turn leads to increased failure load prediction, especially in confined problems such as bearing capacity (e.g. Griffiths 1982). Slope stability analysis, especially with long slopes, is relatively unconfined, thus the choice of dilation angle is less important (Griffiths and Marquez, 2007). As the main objective of the current study is the accurate prediction of slope factors of safety, a compromise value of $\psi = 0$, corresponding to a non-associated flow rule with zero volume change during yield, has been used throughout this paper. This value of ψ enables the model to give reliable factors of safety and a reasonable indication of the location and shape of the potential failure surfaces.

Results

Systematic parameter exploration

For a given slope geometry and set of material properties Figure 4a shows that the *FoS* predicted by the FE method at a *L/H* ratio of 2 is very high, almost double the IS *FoS*. The *FoS* predictions from the FE method decline steeply as the *L/H* ratio increases, so that the IS predictions are within 10% of the FE prediction for *L/H* ratios greater than 10 and within 5 % for *L/H* ratios greater than 12. The FE predictions asymptote at the IS *FoS*. We can use the difference between the FE and IS methods at any given *L/H* ratio as an indicator of the error in the IS method resulting from the assumption of infinite length. We can then use the length at which the IS method predictions fall within 5 or 10% of the FE predictions to calculate a critical *L/H* ratio (L/H_{crit}) at which the assumption of infinite length can be considered reasonable. However, we need to know how general this result is under the range of plausible conditions and which other properties of the slope exert a controlling influence on $L/H_{crit.}$ The systematic parameter exploration provides the data required to address these questions and can most easily be visualised by calculating the difference between IS and FE predictions across the range of *L/H* ratios then normalising this difference as a percentage of the FE *FoS*. The resultant curves are shown in Figure 4b for the unsaturated cases.

<Figure 4 near here>

During the systematic parameter exploration, cohesion appeared to exert the strongest control on the *FoS* difference curves and on the L/H_{crit} value. In fact when cohesion was set to zero the FE predictions did not fall outside 10% of the IS predictions even at the shortest *L/H* ratio (4). Examining the deformed post failure mesh for cohesionless soils within the FE method revealed that they fail in the top layer of elements (Figure 5a). This result fits closely with the IS method for cohesionless soils, which assumes that failure is equally likely at all depths. In this case we would expect failure at an infinitely shallow depth where the additional reinforcement at the toe would be least, the length / depth ratio would be infinite and the infinite length assumption would be most completely fulfilled. In the FE scheme, failure at an infinitely small depth would be represented as failure in the top layer of elements (Figure 5a) but this makes the results difficult to interpret in terms of critical *L/H* values since in this case *L/H* will always be infinite independent of the domain dimensions and any departure from this will be a function of the discretisation of the domain. As a result, we modified our sampling to sample three further cohesions: a negligible but non zero cohesion (0.1 kPa); a very low cohesion (1 kPa) and a midpoint between the two previous cohesion limits (10 kPa).

<Figure 5 near here>

Increasing cohesion slightly to 0.1 kPa forces the failure plane down below the first row of elements (Figure 5b) but not always to the full depth of the model domain. In this situation the FE method captures the competing effects of: additional downslope driving force with depth (represented in the IS method); but also additional reinforcement with depth at the downslope margin of the landslide. As a result, the FE model's failure plane depth differs from the IS prediction, which is always at the base of the domain for cohesive soils. These FE model runs provide reliable L/H_{crit} predictions that are often very small (Figure 4b), immediately suggesting that the L/H_{crit} value provided by Griffiths

et al. (2011) is only one example of a range of possible values and that varying slope properties leads to different L/H_{crit} values.

Increasing the cohesion further to 1 kPa we find that the failure plane is now forced down to the base of the model domain (Figure 5c). For these slope properties the curve is much steeper and more similar to the results reported by Griffiths *et al*. (2011) (Figure 4b). Further increases in cohesion, to 10 kPa (a relatively high value for colluvial soils; see Hammond *et al*., 1992), result in only small changes to the form of the failure (Figure 5d) and to the L/H_{crit} value (Figure 4b). Figure 4b shows the form of the *FoS* difference curves at the limits of the slope properties but is difficult to interpret in terms of the influence of individual parameters on the L/H_{crit} value because: 1) it only shows results for the extremes; and 2) the parameter combinations are difficult to differentiate. We address these limitations using the random parameter exploration.

Random Parameter Exploration

The results from the random parameter exploration are displayed as a series of scatter plots in Figure 6. The patterns for each parameter are similar for convergence at 5 and 10% thresholds but with a lower maximum L/H_{crit} value for the 10% than the 5% threshold. They show that for almost all parameter combinations the IS predictions converge to within 5 and 10% of those from the FE method at *L/H* ratios of no more than 25 and 18 respectively.

<Figure 6 near here>

Of the six infinite slope parameters L/H_{crit} appears most sensitive to slope angle, with a strong negative trend to the upper L/H_{crit} limit with slope. L/H_{crit} is also sensitive to, soil depth, normalised free surface height and friction angle. There are strong negative trends to the upper L/H_{crit} limit for, friction angle and soil depth and nonlinear negative trends to the lower L/H_{crit} limit for soil depth and normalised free surface height so that low L/H_{crit} values are only possible for soils deeper than 1 m

and normalised free surface heights greater than 0.2. Increasing cohesion from very low values causes a rapid nonlinear increase in the upper L/H_{crit} limit. The highest L/H_{crit} values are associated with high cohesion; and low soil depth, slope angle and friction angle; the lowest L/H_{crit} values are associated with low cohesion; and high soil depth, normalised free surface height and slope angle.

Discussion

Critical length depth ratio

Both the systematic and random parameter explorations confirm that the *FoS* predictions from the FE method converge on those of the IS method across the full range of slope properties and geometries that we might find in a catchment. The critical length depth ratio (L/H_{crit}) at which the FE predictions converge to within 5 or 10% of the IS predictions varies with friction angle, cohesion, soil depth, normalised free surface height and slope angle but is insensitive to soil unit weight. For a 5% threshold, L/H_{crit} values can range from 4 (effectively the detection limit for our study) to 25 and for a 10% threshold they vary from 4 to 18.

Slope angle appears the dominant control on the upper limit to L/H_{crit} values. This is perhaps unsurprising given that our definitions of length and depth are planimetric and vertical respectively. As slope angle (β) increases the true length (L_t) increases relative to the planimetric length (L_p) according to: $L_p = L_t / \cos(\beta)$ while the true (slope perpendicular) depth (H_t) decreases relative to the vertical depth (H_v) according to: $H_t = H_v \, 1/\cos(\beta)$. As a result the true length depth ratio (L_t/H_t) is related to the planimetric length depth ratio (L_p/H_v) according to $L_t/H_t = L_p/H_v \, (1/\cos^2(\beta))$. The decrease in L/H_{crit} with slope angle closely follows the expected decrease resulting from this difference between true and planimetric dimensions (grey lines in Figure 6). Despite this, we have continued to use planimetric lengths and vertical depths since these are the dimensions commonly used within catchment slope stability models. Much of the remaining variability is related to the proportion of the soil strength made up by cohesion. We know from Figure 4 and Figure 5 that the lowest L/H_{crit} values will always be found in cohesionless soils; and from Figure 6 that shallow soils

with high cohesion have higher L/H_{crit} values. However, even the steep (>30°), shallow (<1 m), low cohesion (<5 kPa) and high friction (>30°) soils commonly found in upland catchments show a relatively broad range of L/H_{crit} values (5-15 at 10% and 5-20 at 5%). With generalisation to all site properties considered the infinite length assumption within the IS method results in errors of less than 10% for *L/H* ratios greater than 18 and less than 5% for *L/H* ratios greater than 25 (Figure 6). This has important implications for slope stability modelling using the infinite slope method and we will explore these in detail in the following section.

Implications for geomorphic and landscape evolution models

Catchment landslide models solve the infinite slope equation for each cell in a mesh. They assume implicitly that the (downslope) length and (across slope) width of these cells represent the dimensions of the predicted landslide (Dietrich *et al*., 2008) and that these dimensions are large enough relative to the failure plane that the infinite slope assumption is valid (Ray *et al*., 2010). Our results suggest that the infinite length assumption is valid, and results in less than 5% error for landslides (and therefore model cells) with *L/H* ratios greater than 25 independent of material properties. This validity will hold provided the grid resolution is more than 25 times the expected failure plane depth. For example, many studies use a spatially constant failure plane depth of ~1m (e.g. Montgomery and Deitrich, 1994; Wu and Sidle, 1995). In this case, models with a grid resolution of 25 m or more can apply the infinite slope method without significant length effects. However, for models with a cell size less than 25 times the assumed landslide failure plane depth, edge effects become possible and are likely to be significant if the length / depth ratio drops below 8. In these cases many of the IS predictions differed from the FE predictions by greater than 50%. Assuming failures of equal length and width, with a 1 m depth, this would mean that even groups of ~60 1 m resolution cells are likely to be predicted as 50% less stable than they should be as a result of length effects not represented by the infinite slope method. The dependence of the validity of the infinite slope model upon cell size emphasises that care is required in assuming that higher resolution topographic data always improve identification of landslide risk. Although the coarser cell

size may result in error because of the minimum landslide area that can be identified, higher resolution data may result in error since the identified landslides may violate the infinite slope length assumption.

To demonstrate the implications that this has for a catchment scale stability model we applied a simple grid based stability model, using photogrammetrically derived topographic data (Milledge *et al*., 2009), to produce a set of predicted landslides for a 1 km^2 study area in the English Lake District, Northern England (Warburton, *et al*. 2008). As we have discussed above, the main difference in catchment scale stability models is the hydrological treatment used to define the pore water pressure field. There is considerable debate around what drives the pore water pressure increase that triggers landslides, with different groups arguing that it is: dominated by lateral redistribution of water (e.g. Montgomery and Dietrich 1994; 2004; Montgomery *et al*., 2002); dominated by vertical infiltration (e.g. Iverson, 2000; 2004); or a combination of these (e.g. D'Odorico and Fagherazzi, 2003). We will give an example for the simple and widely used case where the pore water pressure field is driven by lateral redistribution. To do this we applied SHALSTAB (Dietrich and Montgomery, 1998) in a deterministic sense (i.e. for a defined rainfall and transmissivity). This model setup is analogous to the stability treatment within those landscape evolution models that attempt to model hydrologically triggered landslides (e.g. Tucker and Bras, 1998). While it is very simple, its basis around the topographic control on spatial soil moisture is very common (e.g. Wu and Sidle, 1995; Burton and Bathurst, 1998; Pack *et al*., 1998; Borga *et al*., 2002; Vanacker *et al*., 2003; Dhakal and Sidle, 2004; Reid *et al*., 2007; Simoni *et al*., 2008; for exceptions see: Iverson, 2000; Baum *et al*., 2008).

We ran the model to predict landslides in two different scenarios: 1) the most common scenario, using a coarse (10 m) grid resolution since this is a resolution typical of the most widely available topographic data; and 2) the increasingly common scenario of finer (1 m) grid resolution to take advantage of the constantly improving topographic data.

<Figure 7 near here>

Existing research has highlighted the influence of grid resolution on this type of model (e.g. Dietrich and Montgomery, 1998; Claessens *et al.*, 2005). Our predicted landslides have characteristics that are consistent with previous findings, particularly that new areas of potential instability are identified at finer resolution (e.g. upper left corner of the Figure 7b). These relate to improved topographic representation, which captures small steep areas that were previously smoothed out at the coarser resolution. We also find that many of the predicted landslides are long for both the high and low resolution model runs. The hydrological model generates patches of high pore water pressure that are long in a downslope direction. As a result the model predicts long landslides and with high *L/H* ratios that minimise the error associated with using the IS method. This suggests that the IS method can applied in this case with high resolution data without violating its infinite length assumption. It is worth noting that these long zones of predicted instability are a function of the model's assumption that lateral redistribution drives pore water pressure patterns. It is the underlying hydrological processes that drive characteristic *L/H* ratios; and these produce slides with *L/H* ratios that do not violate the infinite slope stability assumption in this case. This suggests that the acceptability of the IS model depends not only on data resolution but also on catchment hydrology and its representation in the landslide model. Models with different hydrological representation might produce zones of instability with different geometries, although lateral redistribution remains important control through its influence on antecedent pore water pressures (Iverson, 2000; Montgomery and Dietrich, 2004). The suitability of these models will need to be assessed with reference to our findings on the critical *L/H* ratio at which the IS method becomes applicable. Critically, our results do not give a single answer on the suitability of the IS method for geomorphological slope stability modelling, but they provide a tool to assess its suitability on a case by case basis, something that should be a routine part of testing these models.

While finer grid resolutions still predict long landslides the predicted width is dramatically reduced. This prompts an important question: how reasonable is the assumption of infinite width and what are

the critical width depth ratios at which the infinite slope assumptions break down? This question cannot be addressed using the 2D finite element geotechnical model used in this study, since it also assumes a slope of infinite width. Instead, solving this question would require a similar research design within a 3D model, such models exist and research to address this question is underway.

Conclusion

Factor of safety predictions from the Finite Element method always converge to within 5 % of those from the infinite slope method when the length / depth ratio exceeds 25. However, they can converge at much lower length / depth ratios depending on the geometry and material properties of the slope. The critical length depth ratio at which the predictions converge is in part controlled by the proportion of the soil strength that comes from cohesion rather than from friction with the longer length depth ratios required for more cohesive soils and very rapid convergence at low length depth ratios for low cohesion soils.

The infinite length assumption within the infinite slope method is valid for many of the existing modelling studies, which have used a coarse (>25 m) resolution. For models with a finer resolution (<10 m) the assumption of infinite length might be less valid depending on the assumed landslide failure plane depth and on the material properties. However, if lateral subsurface flow plays a role in defining pore water pressure then its spatial organisation mitigates against predicting short landslides and minimises the risk that predicted landslides will have length depth ratios less than 25.

In this case, whilst it is unlikely that the infinite length assumption introduces error into the stability predictions because modelled landslides are often long, the infinite width assumption is more likely to be violated since predicted landslides get narrower as the grid resolution is reduced. It may be width and not length that limits the applicability of the infinite slope method and maintains the stability of potential landslides. This is a topic that requires further research since it is not tractable within a standard 2D geotechnical profile treatment but requires a 3D approach.

Acknowledgements

Data used as part of this research were funded by NERC Research Grant NE/D521481/1 to JW. DGM was funded by NERC PhD Studentship NER/S/A/2004/12248 and NERC Fellowship NE/H015949/1.

References

Bathurst JC, Moretti G, El-Hames A, Moaven-Hashemi A, Burton A. 2005. Scenario modelling of basin-scale, shallow landslide sediment yield, Valsassina, Italian Southern Alps. *Natural Hazards and Earth System Sciences* **5**: 189-202.

Baum RL, Savage WZ, Godt JW. 2008. TRIGRS - a fortran program for transient rainfall infiltration and grid-based regional slope stability analysis, version 2.0. In, *Open File Report* (p. 81): U.S. Geological Survey.

Borga M, Dalla Fontana G, Gregoretti C, Marchi L. 2002. Assessment of shallow landsliding by using a physically based model of hillslope stability. *Hydrological Processes* **16**: 2833-2851.

Burton A, Bathurst JC. 1998. Physically based modelling of shallow landslide sediment yield at a catchment scale. *Environmental Geology* **35**: 89-99.

Casadei M, Dietrich WE, Miller NL. 2003. Testing a model for predicting the timing and location of shallow landslide initiation in soil-mantled landscapes. *Earth Surface Processes and Landforms* **28**: 925-950.

Chugh AK. 2003. On the boundary conditions in slope stability analysis. *International Journal for Numerical and Analytical Methods in Geomechanics* **27**: 905–926.

Claessens L, Heuvelink GBM, Schoorl JM, Veldkamp A. 2005. DEM resolution effects on shallow landslide hazard and soil redistribution modelling. *Earth Surface Processes and Landforms* **30(4)**: 461–477, doi: 10.1002/esp.1155

Crosta GB, Frattini P. 2003. Distributed modelling of shallow landslides triggered by intense rainfall. *Nat. Hazards Earth Syst. Sci.* **3**: 81-93.

Dhakal AS, Sidle RC. 2004. Distributed simulations of landslides for different rainfall conditions. *Hydrological Processes* **18**: 757-776.

Dietrich WE, McKean J, Bellugi D, Perron T. 2008. The prediction of shallow landslide location and size using a multidimensional landslide analysis in a digital terrain model. In *Fourth International Conference on Debris-Flow Hazards Mitigation: Mechanics, Prediction, and Assessment (DFHM-4), Chengdu, China, September 10-13, 2007*, Chen CL, Major JJ (eds). Amsterdam: IOS Press.

Dietrich WE, Montgomery DR. 1998. SHALSTAB: a digital terrain model for mapping shallow landslide potential. In, *Technical Report* (p. 29): NCASI.

D'Odorico P, Fagherazzi S. 2003. A probabilistic model of rainfall-triggered shallow landslides in hollows: A long-term analysis, *Water Resources Research*. **39**: 1262, doi:10.1029/2002WR001595.

Gabet EJ, Dunne T. 2002. Landslides on coastal sage-scrub and grassland hillslopes in a severe El Nino winter: The effects of vegetation conversion on sediment delivery. *Geological Society of America Bulletin* **114**: 983-990.

Griffiths DV. 1982. Computation of bearing capacity factors using finite elements. *Geotechnique* **32(3)**: 195–202.

Griffiths DV, Huang JS, Dewolfe GF. 2011. Numerical and analytical observations on long and infinite slopes. *International Journal for Numerical and Analytical Methods in Geomechanics* **35**: 569-585.

Griffiths DV, Lane PA. 1999. Slope stability analysis by finite elements. *Geotechnique* **49**: 387-403.

Griffiths DV, Marquez RM. 2007. Three-dimensional slope stability analysis by elasto-plastic finite elements. *Geotechnique* **57**: 537-546.

Haefeli R. 1948. The stability of slopes acted upon by parallel seepage. In *International Conference on Soil Mechanics and Foundation Engineering*; 57-62.

Hammah RE, Yacoub TE, Corkum B, Curran JH. 2005. A comparison of finite element slope stability analysis with conventional limit-equilibrium investigation. In *58th Canadian Geotechnical*

and 6th Joint IAH-CNC and CGS Groundwater Specialty Conferences - GeoSask 2005. Saskatoon; 480-487.

Haneberg WC. 2004. A rational probabilistic method for spatially distributed landslide hazard assessment. *Environmental & Engineering Geoscience* **10**: 27-43.

Iverson RM. 2000. Lanslide triggering by rain infiltration. *Water Resources Research* **36**: 1897-1910.

Iverson RM. 2004. Comment on ‘‘Piezometric response in shallow bedrock at CB1: Implications for runoff generation and landsliding’’ by David R. Montgomery, William E. Dietrich, and John T. Heffner, *Water Resources Research* **40**: W03801, doi:10.1029/2003WR002077.

Larsen IJ, Montgomery DR, Korup O. 2010. Landslide erosion controlled by hillslope material. *Nature Geosci* **3**: 247-251.

Milledge DG. 2009. Digital filtering of generic topographic data in geomorphological research. *Earth Surface Processes and Landforms* **34**: 63-74.

Montgomery DR, Dietrich WE. 1994. A Physically-Based Model for the Topographic Control on Shallow Landsliding. *Water Resources Research* **30**: 1153-1171.

Montgomery DR, Dietrich WE, Heffner JT. 2002. Piezometric response in shallow bedrock at CB1: Implications for runoff generation and landsliding, *Water Resources Research.* **38**(12): 1274, doi:10.1029/ 2002WR001429.

Montgomery DR, Dietrich WE. 2004. Reply to comment by Richard M. Iverson on ‘‘Piezometric response in shallow bedrock at CB1: Implications for runoff generation and landsliding,’’ *Water Resources Research* **40:** W03802, doi:10.1029/2003WR002815.

Pack RT, Tarboton DG, Goodwin CN. 1998. The SINMAP approach to terrain stability mapping In, *8th International Congress of the International Association for Engineering Geology and the Environment*. Vancouver, Canada.

Perzyna P. 1966. Fundamental problems in viscoplasticity. *Advances in Applied Mechanics* **9**: 243–377.

Ray RL, Jacobs JM, de Alba P. 2010. Impacts of Unsaturated Zone Soil Moisture and Groundwater Table on Slope Instability. *Journal of Geotechnical and Geoenvironmental Engineering* **136**: 1448-1458.

Reid SC, Lane SN, Montgomery DR, Brookes CJ. 2007. Does hydrological connectivity improve modelling of coarse sediment delivery in upland environments? *Geomorphology* **90**: 263-282.

Simoni S, Zanotti G, Bertoldi G, Rigon R. 2008. Modelling the probability of occurence of shallow landslides and channelized debris flows using GEOtop-FS. *Hydrological Processes* **22**: 2248-2263.

Skempton AW, DeLory FA. 1957. Stability of natural slopes in London clay. In *4th International Conference on Soil Mechanics and Foundation Engineering*; 378-381.

Taylor DW. 1948. *Fundamentals of Soil Mechanics*. Wiley: New York.

Tucker GE, Bras RL. 1998. Hillslope processes, drainage density, and landscape morphology. *Water Resources Research* **34**: 2751-2764.

Vanacker V, Vanderschaeghe M, Govers G, Willems E, Poesen J, Deckers J, De Bievre B. 2003. Linking hydrological, infinite slope stability and land-use change models through GIS for assessing the impact of deforestation on slope stability in high Andean watersheds *Geomorphology* **52**: 299-315.

Warburton J, Milledge DG, Johnson RM. 2008. Assessment of shallow landslide activity following the January 2005 storm, Northern Cumbria. *Proceedings of the Cumberland Geological Society* **7**: 263-283.

Wu WM, Sidle RC. 1995. A Distributed Slope Stability Model for Steep Forested Basins. *Water Resources Research* **31**: 2097-2110.

Zienkiewicz OC, Humpheson C, Lewis RW. 1975. Associated and Non-Associated Visco-Plasticity and Plasticity in Soil Mechanics. *Geotechnique* **25**: 671-689.

Tables

Table 1: Parameters varied within the parameter exploration with the range over which they were varied. Young's Modulus and Poisson's Ratio were held constant at the values below.

Parameter	Value Range
Friction Angle (φ')	15 - 45°
Cohesion (c')	0 - 20 kPa
Soil Depth (H)	0 - 3 m
Normalised free surface height (m)	0 - 1
Soil Unit Weight (γ_{sat})	1.1 - 1.8 kN m^{-3}
Slope Angle (β)	15 - 45°
Young's Modulus	10^5 kPa
Poisson's Ratio	0.3

Figures

Figure 1: Cumulative probability distributions for the length / depth ratios of landslides from two inventories in Cumbria, UK (Warburton *et al.*, 2008) and and California, USA (Gabet and Dunne, 2003).

Figure 2: Schematic profile view through an infinite slope showing the relevant forces and lengths.

Figure 3: example finite element mesh of 8-node quadrilateral elements annotated to show the relevant lengths and angles used within the model.

Figure 4: A) relationship between length / depth ratio and factor of safety for infinite slope (IS) and finite element (FE) models for an example slope with φ'=30 °, c'=20 kPa, γ_{sat}=19 kN m^3, H =5 m and β=25 °; B) difference between FE and IS predictions (expressed as a percentage of FE *FoS*) for different length / depth ratios.

Figure 5: deformed meshes showing the shape of the failure mechanism for a slope with φ'=20 °, γ_{sat}=1.9kN m^{-3}, m = 0, L = 2 m, H = 0.5 m, β=20 ° and cohesions of: A) 0 kPa, B) 0.1 kPa, C) 1 kPa, and D) 10 kPa. Displacements are exaggerated for visualisation and should be interpreted as relative rather than absolute.

Figure 6: uncertainty plots showing variation in the length / depth ratio at which the infinite slope predictions converge to within 5 and 10% of the finite element predictions (L/H_{crit}) for a range of: friction angles, soil cohesions, soil depths, normalised free surface heights, soil unit weights and slope angles. The bottom row shows results for parameters sampled to zero in semi-logarithmic space to illustrate their influence at low values. The grey lines on the slope angle plots have the equation y = a $\cos^2(\beta)$, where a = 24 and 16 for the upper and lower plots respectively.

Figure 7: predicted landslides from a 1 km^2 patch of a grid based stability model with φ'=40 °, c'=1 kPa, γ_{sat}=1.7 kN m^{-3}, transmissivity = 0.01 mm h^{-1} and steady state rainfall rate = 100 mm h^{-1}, H = 1 m, cellsize is 10 m for a and 1 m for b.

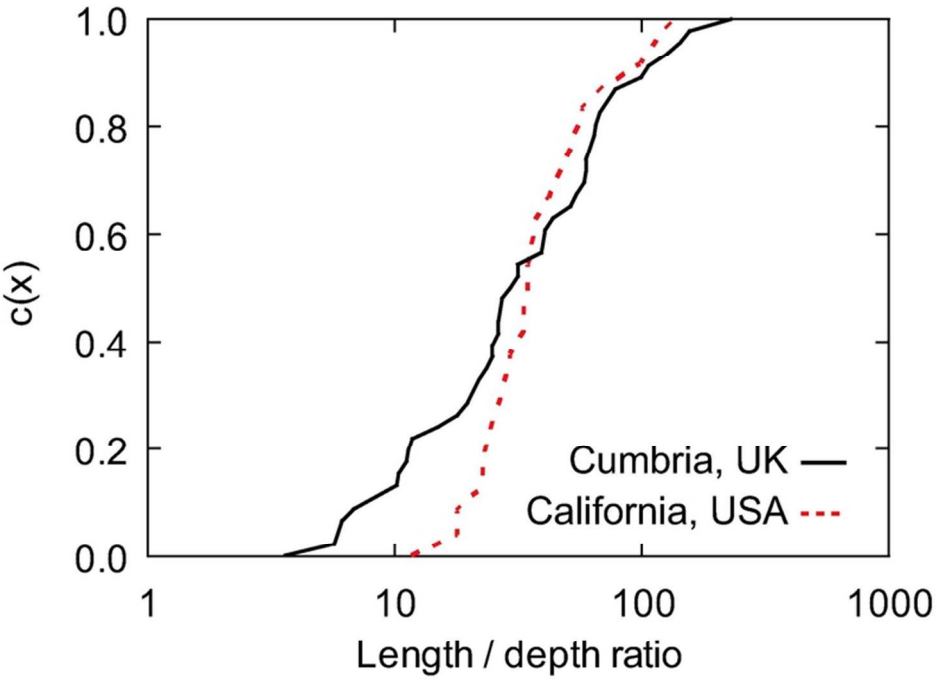

Figure 1: Cumulative probability distributions for the length / depth ratios of landslides from two inventories in Cumbria, UK (Warburton et al., 2008) and and California, USA (Gabet and Dunne, 2003).
71x55mm (300 x 300 DPI)

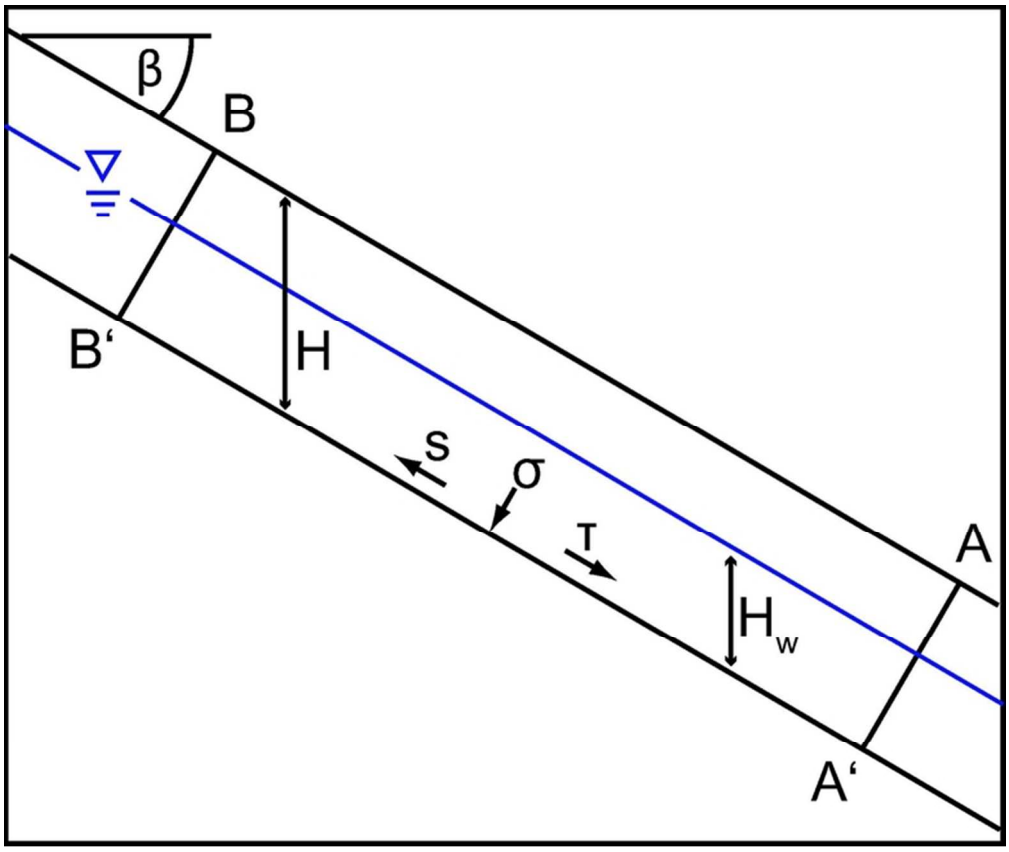

Figure 2: Schematic profile view through an infinite slope showing the relevant forces and lengths.
65x55mm (300 x 300 DPI)

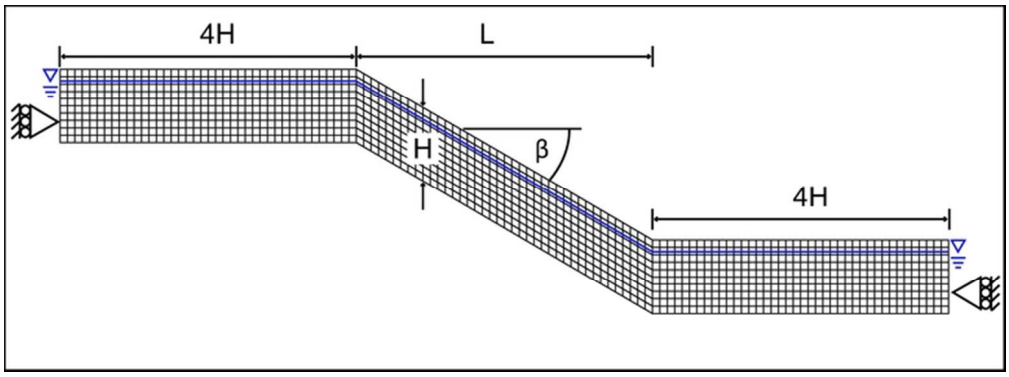

Figure 3: example finite element mesh of 8-node quadrilateral elements annotated to show the relevant lengths and angles used within the model.
65x24mm (300 x 300 DPI)

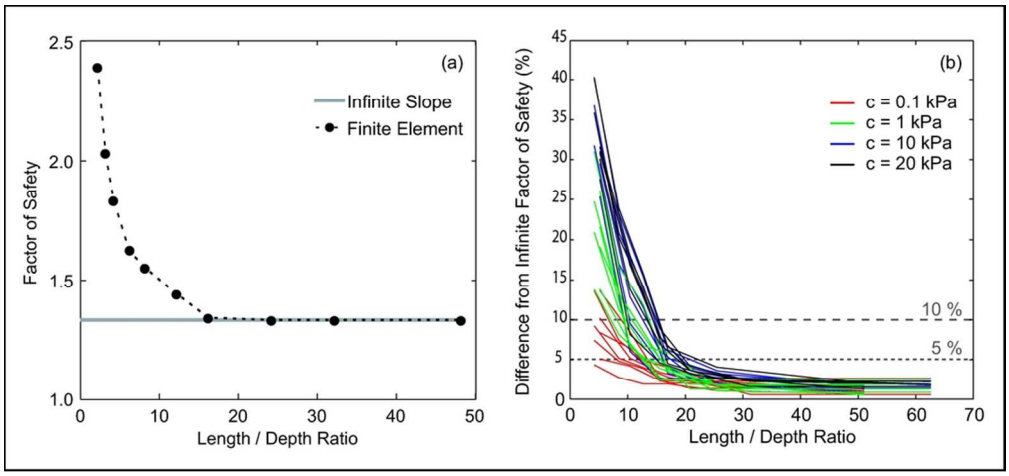

Figure 4: A) relationship between length / depth ratio and factor of safety for infinite slope (IS) and finite element (FE) models for an example slope with φ'=30 °, c'=20 kPa, γsat=19 kN m3, H =5 m and β=25 °; B) difference between FE and IS predictions (expressed as a percentage of FE FoS) for different length / depth ratios.
90x42mm (300 x 300 DPI)

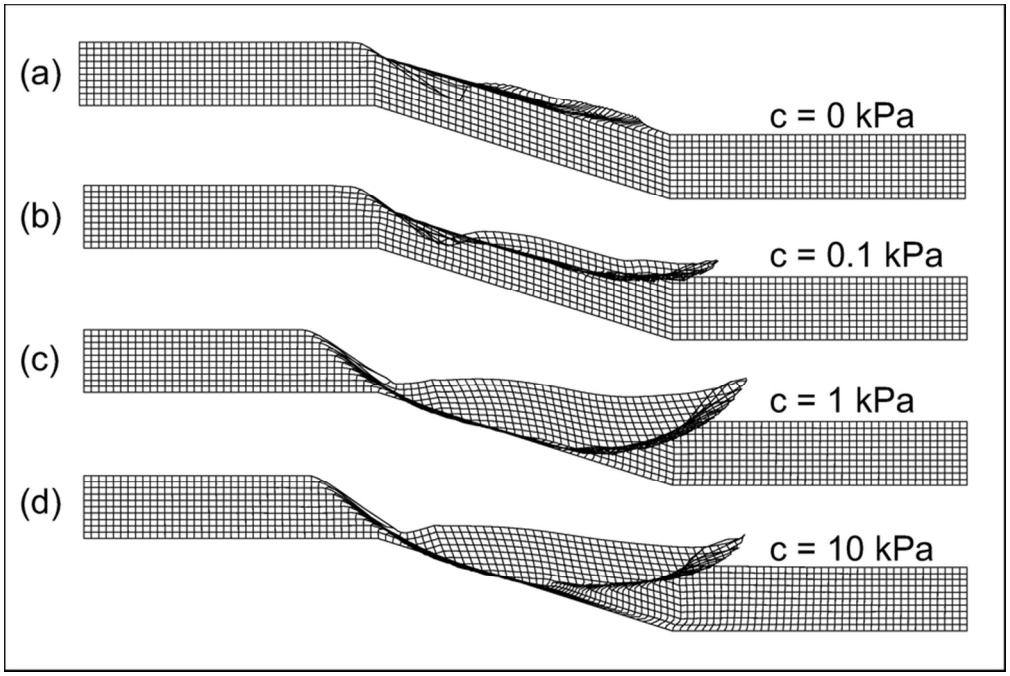

Figure 5: deformed meshes showing the shape of the failure mechanism for a slope with φ'=20 °, γsat=1.9kN m-3, m = 0, L = 2 m, H = 0.5 m, β=20 ° and cohesions of: A) 0 kPa, B) 0.1 kPa, C) 1 kPa, and D) 10 kPa. Displacements are exaggerated for visualisation and should be interpreted as relative rather than absolute.
81x54mm (300 x 300 DPI)

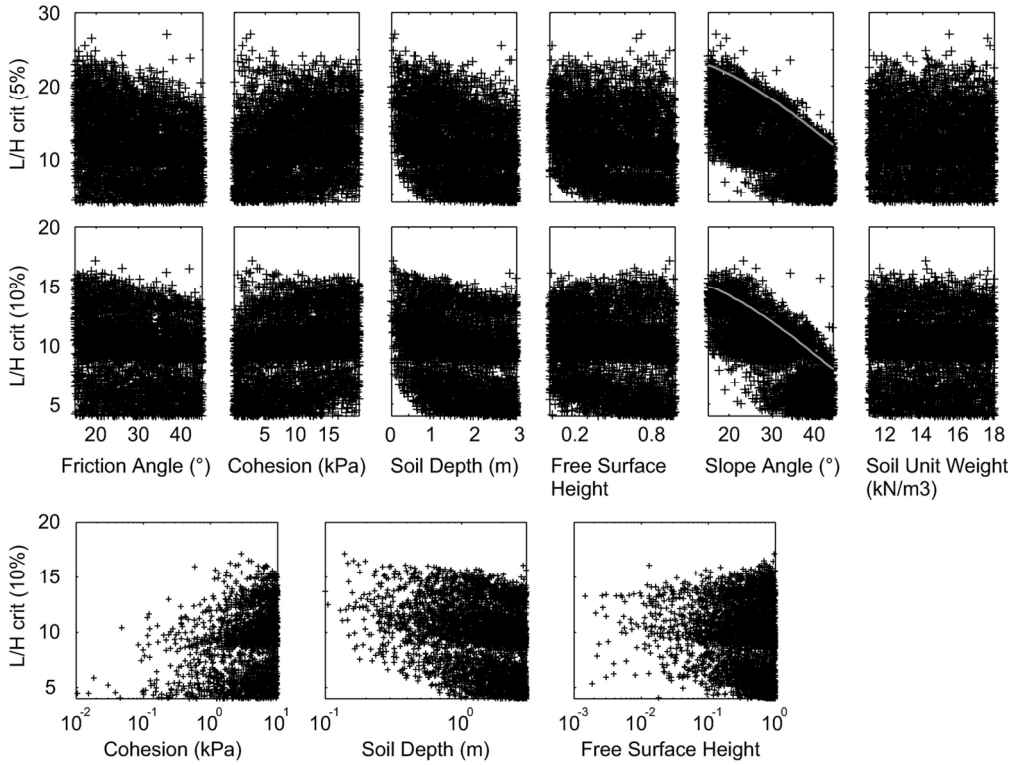

Figure 6: uncertainty plots showing variation in the length / depth ratio at which the infinite slope predictions converge to within 5 and 10% of the finite element predictions (L/Hcrit) for a range of: friction angles, soil cohesions, soil depths, normalised free surface heights, soil unit weights and slope angles. The bottom row shows results for parameters sampled to zero in semi-logarithmic space to illustrate their influence at low values. The grey lines on the slope angle plots have the equation y = a cos2(β), where a = 24 and 16 for the upper and lower plots respectively.
133x101mm (300 x 300 DPI)

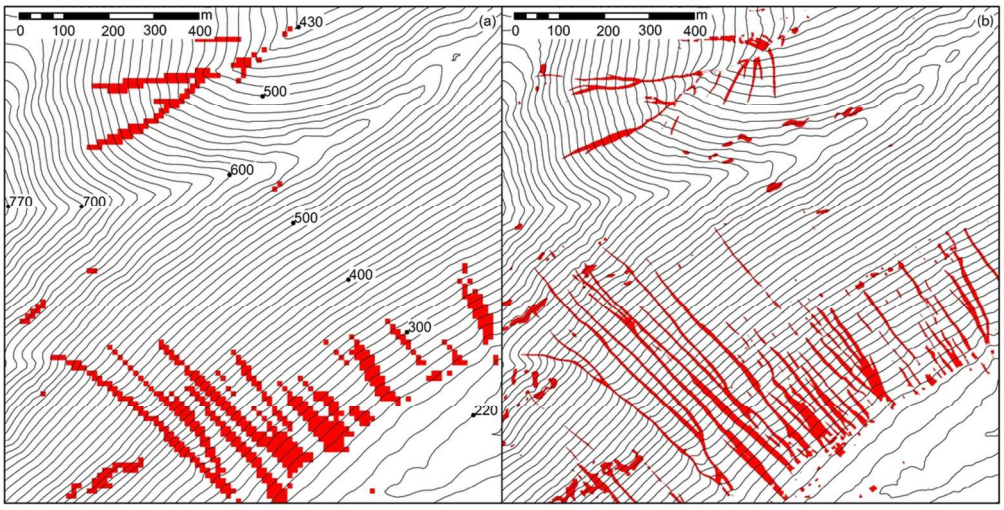

Figure 7: predicted landslides from a 1 km2 patch of a grid based stability model with φ'=40°, c'=1 kPa, γsat=1.7 kN m-3, transmissivity = 0.01 mm h-1 and steady state rainfall rate = 100 mm h-1, H = 1 m, cellsize is 10 m for a and 1 m for b.
100x50mm (300 x 300 DPI)